Journal of Applied Mechanics and Technical Physics, Vol. 42, No. 3, pp. 558–564, 2001

DEVELOPMENT OF THE POLYMERIC SPLIT HOPKINSON BAR TECHNIQUE

A. S. Yunoshev and V. V. Sil'vestrov

UDC 678.01:539.3

A compression version of the split Hopkinson bar with pressure bars and a striker, which are made of Plexiglas (a material with low density and velocity of sound) is developed. The technique is designed to determine stress–strain diagrams under high strain rates of highly deformable materials with low density and strength, such as plastics, foams, and rubbers. Dynamic stress–strain curves in compression for spheroplastic, foam plastic, and rubber are presented, which were obtained using the technique developed.

Introduction. To study the effect of the strain rate $\dot{\varepsilon}$ on the mechanical characteristics of various materials within the strain-rate range of 10^2–10^4 sec^{-1}, the split Hopkinson bar technique is widely used [1–4]. To study the dynamic behavior of viscoelastic plastics with an acoustic impedance $I = \rho c \geqslant 1$ MPa · sec/m (ρ is the density of the bar material and c is the velocity of sound in the bar), the pressure bars are made of aluminum alloys with an impedance of 14 MPa · sec/m. However, aluminum and other materials with $I \sim 10$ MPa · sec/m are not suitable for testing materials with an impedance of the order of 0.1 MPa · sec/m. Two problems arise in studying more compliant polymeric and porous materials, which are low-strength and low-density substances with ultimate strains reaching 50% and more. First, the amplitude of the transmitted wave is small because of the large difference in acoustic impedances of the pressure bars and the material under study, and there arises the problem of registration of the transmitted wave on the background of the noise of the registering system. Second, in metallic pressure bars used in polymer studies, the ultimate strain is not generally reached because the duration of the incident pulse is limited by the finite length of the striker and the high velocity of sound $c \approx 5$ km/sec in the striker material. To determine the ultimate strain, one has to increase the duration of the compression pulse, which results in a significant increase in the lengths of the striker and input and output bars and which is associated with technological difficulties (manufacturing of pressure bars 2 to 3 meters long and throwing of a striker 0.5 to 1 m long with a velocity of 5 to 20 m/sec).

A possible solution of these problems was proposed in [5, 6]. It implies the use of the split Hopkinson bar technique with pressure bars and a striker, which are made from a material with a density $\rho \approx 1$ g/cm^3 and a velocity of sound $c \approx 1.5$–2 km/sec, i.e., two or three times lower than that in metals. For an identical duration of the incident pulse, this leads to a threefold reduction of the lengths of the striker and pressure bars; for an identical length of the facility, this leads to a threefold increase in the incident pulse duration. The acoustic impedance of the material of the pressure bars decreases approximately by an order of magnitude, and the amplitude of the transmitted wave significantly increases. As a result, dynamic deformation of low-density materials may be studied in the case of high strains.

If the pressure bars are made of polymeric materials, the problem of description of dynamic deformation of the bar material arises, since simple equations of elasticity are inapplicable here. It is necessary to use more complicated viscoelastic models that take into account the effect of the strain rate on mechanical stresses. Note that the wave propagation in polymeric bars is accompanied by significant wave decay with an attenuation factor $\alpha \approx 0.1$–1 m^{-1}. As a result, the strain signal measured by the strain gauge at the point of its location on the bar

Lavrent'ev Institute of Hydrodynamics, Siberian Division, Russian Academy of Sciences, Novosibirsk 630090.
Translated from Prikladnaya Mekhanika i Tekhnicheskaya Fizika, Vol. 42, No. 3, pp. 212–220, May–June, 2001. Original article submitted October 16, 2000.

 0021-8944/01/4203-0558 $25.00

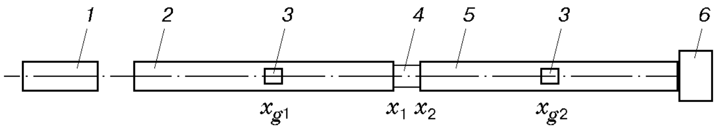

Fig. 1. Scheme of the split Hopkinson bar: 1) striker; 2) incident bar; 3) strain gauges; 4) specimen of the material examined; 5) transmitter bar; 6) damping stop.

does not coincide with the strain profile at the bar/specimen interface, i.e., at the place where the specimen of the material examined is located. The stress and particle velocity in the wave cannot be determined by multiplication of strain by a constant. In this case, to construct the σ–ε diagram of the materials examined, one has to use general relations of the split Hopkinson bar technique. This requires the development of a method of reconstruction of stress and velocity profiles at the specimen boundaries from strain-wave profiles measured at a significant distance from the specimen.

Labibes et al. [5] proposed to use the viscoelastic model of a standard linear solid (SLS) to describe wave propagation in polymeric bars. The technique for processing experimental wave profiles obtained using the split Hopkinson bar and the SLS model is described in [6]. This technique was first applied in experiments with the use of pressure bars made of cast polycarbonate ($c \approx 1.5$ km/sec) [7, 8]. For the pressure-bar lengths of 2.5 m and the striker length of 1.07 m, a loading duration up to 1400 μsec was obtained, and a 50–80% dynamic deformation was obtained in compression of polycarbonate and highly porous materials with a density of 0.05–1.2 g/cm^3 and strength of 1–300 MPa at strain rates of 500–2300 sec^{-1}.

The objective of the present work is to develop the split Hopkinson bar technique with pressure bars made of Plexiglas for testing materials in compression. The bars 920 mm long and 20 mm in diameter were made of SOL Plexiglas (Fig. 1). The stress pulse on the free end of the input bar was generated by the impact of a striker bar made of Plexiglas; the length of the latter was up to 200 mm. Strain pulses in the incident wave had a duration up to 200 μsec and a shape close to a trapezium. Titanium plates 1 mm thick were placed between the specimen of the material examined and the bar ends to prevent the damage of the end faces of the bars in specimen compression. The ends of the specimen were covered by light lubrication to decrease friction [9]. The strain signals on the bars in the sections x_{g1} and x_{g2} located at a distance of 420 mm from the specimen tested were registered by two pairs of foil strain gauges 3 mm long, which were glued at diametrically opposite points and connected in series to compensate for bending waves and were digitized by an eight-channel fast-response L-1211 analog-to-digital converter with the sampling rate up to 1 MHz.

1. General Relations for the Split Hopkinson Bar Technique. The mean dynamic stress in the specimen $\sigma_{\rm s}(t)$ was determined as a half-sum of stresses at the left and right ends of the specimen (sections x_1 and x_2 in Fig. 1):

$$\sigma_{\rm s}(t) = \frac{S_{\rm b}}{2S_{\rm s}}\,[\sigma(x_1,t)+\sigma(x_2,t)] = \frac{S_{\rm b}}{2S_{\rm s}}\,[\sigma_i(x_1,t)+\sigma_{\rm r}(x_1,t)+\sigma_{\rm t}(x_2,t)]. \tag{1}$$

Here $S_{\rm b}$ and $S_{\rm s}$ are the cross-sectional areas of the bar and the specimen; the subscripts i, r, and t indicate the corresponding quantities of the incident, reflected, and transmitted waves, respectively.

The strain rate of the specimen material $\dot\varepsilon_{\rm s}(t)$ was determined by the difference in the particle velocities $u(x,t)$ of the left and right butt ends of the specimen:

$$\dot\varepsilon_{\rm s}(t) = (u(x_2,t)-u(x_1,t))/l_{\rm s} = (u_{\rm t}(x_2,t)-u_i(x_1,t)-u_{\rm r}(x_1,t))/l_{\rm s} \tag{2}$$

($l_{\rm s}$ is the initial length of the specimen).

The strain was calculated by the formula

$$\varepsilon_{\rm s}(t) = \int_0^t \dot\varepsilon_{\rm s}(t)\,dt = \frac{1}{l_{\rm s}}\int_0^t [u_{\rm t}(x_2,t)-u_i(x_1,t)-u_{\rm r}(x_1,t)]\,dt. \tag{3}$$

Eliminating the time t from Eqs. (1) and (3), we obtain the sought dynamic σ–ε diagram for the material examined at a strain rate determined by Eq. (2). Note that the profiles of three waves (incident, reflected, and transmitted ones) are used in Eqs. (1)–(3) in the general case.

The stress and velocity profiles in Eqs. (1)–(3) correspond to sections at the ends of the specimen. The strain profiles are determined in the experiment at a distance of at least ten diameters of the bars from the

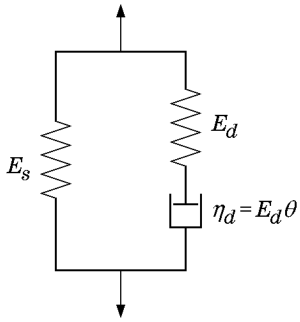

Fig. 2. Mechanical model of a standard linear solid.

sections x_1 and x_2. For elastic metal bars, wave profiles do not change significantly as the waves propagate from the measurement points to the point where the specimen is located, and the elastic linear solid approximation is used to describe wave propagation. In this case, Eqs. (1)–(3) are significantly simplified and may be written in terms of strain.

For bars made of a polymeric material, a significant change in the strain profiles due to viscoelastic effects is observed. Therefore, one has to reconstruct the velocities and stresses at the butt ends of the specimen from experimental strain signals registered at a large distance from the specimen location.

To solve the problem of propagation of a viscoelastic wave in a polymeric bar, the equations of motion and continuity should be supplemented by a constitutive equation relating the mechanical stress σ and strain ε. For instance, for the mechanical model of a standard linear solid consisting of an elastic element and a Maxwell element connected in parallel (Fig. 2), these equations have the following form [1, 2]:

$$\rho_0 \frac{\partial u}{\partial t} = \frac{\partial \sigma}{\partial x}; \tag{4}$$

$$\frac{\partial u}{\partial x} = \frac{\partial \varepsilon}{\partial t}; \tag{5}$$

$$\frac{\partial \sigma}{\partial t} + \frac{\sigma}{\theta} = (E_{\rm s} + E_{\rm d}) \frac{\partial \varepsilon}{\partial t} + \frac{E_{\rm s}}{\theta} \varepsilon. \tag{6}$$

Equation (6) is written in the approximation of comparatively weak waves for which the strain does not exceed 1–2% and the effects of nonlinear elasticity are insignificant [5]. The elasticity modulus $E_{\rm s}$ is determined on the basis of standard quasi-static measurements [10]. The chosen viscoelastic model includes only one Maxwell element and, hence, one relaxation time θ and one value of the dynamic elastic constant $E_{\rm d}$. These approximations correspond to the conditions of the split Hopkinson bar technique but require verification, which is one of the goals of the present work.

To determine the model parameters $E_{\rm d}$ and θ, we use the special solution of system (4)–(6), which is a travelling wave with an exponentially decreasing amplitude [1, 6]: $f(x,t) = A\exp(\pm\alpha x)\exp(i(\omega t \pm kx))$. In the general case, the attenuating factor α and the wavenumber k are functions of the frequency ω, which is a consequence of dispersion and dissipation of waves in viscoelastic bars. It is of interest to consider the high-frequency approximation $\omega \gg 1/\theta$, which corresponds to high strain-rate tests. The phase velocity C for high-frequency waves is independent of ω and equals the velocity of elastic waves C_v for the model with two elastic parallel elements:

$$C^2 = \omega^2/k^2 = (E_{\rm s} + E_{\rm d})/\rho = C_v^2. \tag{7}$$

The attenuating factor may be written in the form

$$\alpha = \frac{E_{\rm d}}{2\theta C_v (E_{\rm s} + E_{\rm d})}. \tag{8}$$

Formulas (7) and (8) relate the dynamic parameters $E_{\rm d}$ and θ for the model of the standard linear solid to the experimentally measured quantities C_v and α.

To calculate the profiles of strain $\varepsilon(x_{g2},t)$, stress $\sigma(x_{g2},t)$, and particle velocity $u(x_{g2},t)$ in the section $x_{g2} > x_{g1}$ from the strain signal $\varepsilon(x_{g1},t)$ in the section x_{g1} by solving Eqs. (4)–(6), we used numerical implementation of the method of characteristics considered in detail in [6].

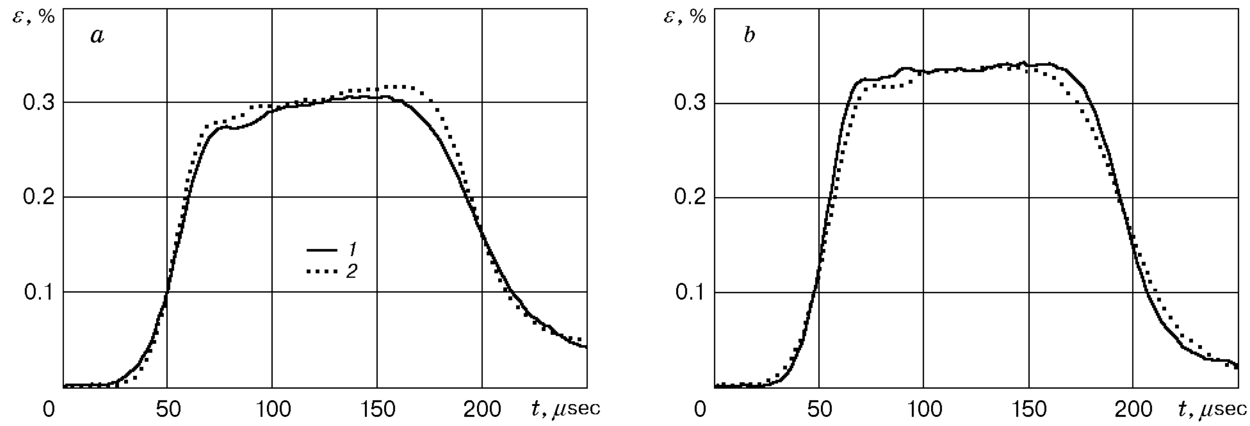

Fig. 3. Example of solving the direct problem in the section x_{g2} (a) and the inverse problem in the section x_{g1} (b): curves 1 and 2 refer to experiment and theory, respectively.

2. Determination of the Parameters of the Standard Linear Solid Model. To determine the dynamic parameters of the SLS model for pressure bars made of Plexiglas, a series of wave-propagation experiments was conducted, where the velocity of perturbations C_v and the attenuating factor α were measured. Knowing these values and also the static elastic constant $E_{\rm s} = 5$ GPa [10], we can calculate the values of the dynamic elastic constant and the stress-relaxation time:

$$E_{\rm d} = C_v^2 \rho_0 - E_{\rm s}, \qquad \theta = E_{\rm d}/[2\alpha C_v(E_{\rm s} + E_{\rm d})].$$

It is shown [11] that, for longitudinal strain-pulse signals propagating in elastic bars, the leading front of the pulse reaches the measurement point before the time z/C_v (z is the distance at which the pulse-shape variation is observed). By the time z/C_v, the strain reaches approximately 1/3 of the final value. Therefore, the propagation velocity of disturbances was measured in the present work as follows. When the striker hit the free end of the input bar, strain signals $\varepsilon(t)$ with an amplitude of approximately 0.5% were registered by two strain gauges located sequentially along the bar at a distance $z = 920$ mm. According to the above considerations, the time interval necessary to calculate C_v was found as the time difference between the points on the leading fronts of strain pulses, which were located at a 1/3-level of the maximum amplitude on the signal.

The attenuating factor was measured using two pulse signals $\varepsilon(t)$. Based on the results of numerical tests for the case of a tapered pulse, we determined the point on the strain pulse, which corresponds to the attenuating factor employed in the algorithm of the method of characteristics and which is located at the intersection of the asymptotes of the leading front and the plateau of the strain signal. Therefore, the experimental calculation of the attenuating factor included determination of the ordinates Y_1 and Y_2 of the points of intersection of the tangent lines to the leading front and plateau for two experimental strain profiles. The value of the attenuating factor was calculated by the formula $\alpha = \ln(Y_1/Y_2)/z$. The thus determined parameters of the SLS model for Plexiglas are $E_{\rm s} = 5$ GPa, $E_{\rm d} = 0.7$ GPa, $C_v = (2.2 \pm 0.1)$ km/sec, $\alpha = (0.2 \pm 0.02)$ m^{-1}, and $\theta = 141$ μsec.

3. Comparison of Experimental Data with Numerical Results. To verify the validity of the chosen model for Plexiglas bars, the calculated strain signals were compared with experimental data $\varepsilon(x_{g1}, t)$ and $\varepsilon(x_{g2}, t)$ registered by strain gauges located in the sections x_{g1} and x_{g2} at a distance of 920 mm. Figure 3a shows the experimental signal $\varepsilon(x_{g2}, t)$ and the calculated profile obtained on the basis of $\varepsilon(x_{g1}, t)$. Figure 3b shows the experimental signal $\varepsilon(x_{g1}, t)$ and the calculated profile obtained on the basis of $\varepsilon(x_{g2}, t)$. The theoretical and experimental strain-pulse signals are in good agreement. Thus, the root-mean-square deviation of the calculated strain profile from the experimental one is less than 3% in solving both the direct (Fig. 3a) and inverse (Fig. 3b) problems.

It follows from the results obtained that the simple viscoelastic SLS model offers a good description of evolution of the strain-pulse signal in the compression wave propagating along a cylindrical bar made of Plexiglas. If the bar material is changed, the model parameters have to be determined again because the model parameters are significantly different even for cast polymethacrylate of different brands.

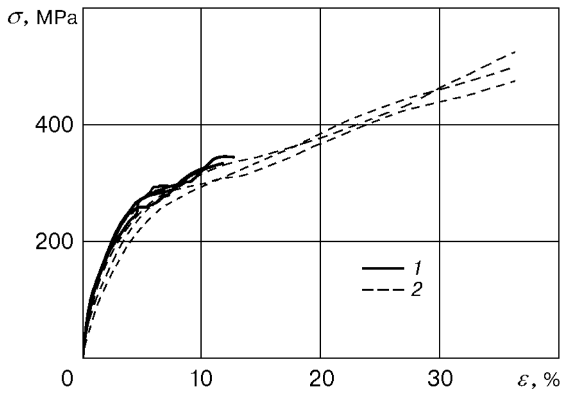

Fig. 4

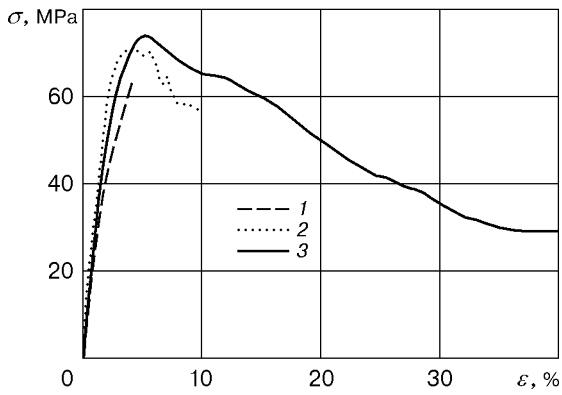

Fig. 5

Fig. 4. Dynamic stress–strain diagrams for D16 Duralumin ($I = 14$ MPa · sec/m) obtained using pressure bars made of steel for $\dot{\varepsilon} \approx 6000$ sec^{-1} (curves 1) and Plexiglas for $\dot{\varepsilon} \approx 2200$ sec^{-1} (curves 2).

Fig. 5. Static diagram (curve 1) and dynamic stress–strain diagrams in compression of spheroplastic ($\dot{\varepsilon} \approx 3000$ sec^{-1} and $I = 1.38$ MPa · sec/m) obtained using pressure bars made of steel (curve 2) and Plexiglas (curve 3).

To check the technique, experiments were conducted for determining the σ–ε diagram of deformation of a material insensitive to the strain rate; steel and Plexiglas pressure bars were used. The independence of $\dot{\varepsilon}$ is important, since the size of the specimens to be tested on steel and Plexiglas bars should be different to obtain close values of $\dot{\varepsilon}$ in both cases because of the different acoustic impedances of metals and polymers. The agreement of results in these cases should confirm the workability of the technique of the split Hopkinson bar with polymeric pressure bars.

In accordance with [3], the σ–ε diagram of aluminum alloys is independent of the strain rate within the range $\dot{\varepsilon} \sim 10^{-6}$–$5 \cdot 10^3$ sec^{-1}. Therefore, D16 Duralumin was chosen as a test material [4]. Based on the above technique, σ–ε diagrams of deformation for Duralumin D16 were obtained. Pressure bars made of steel and Plexiglas were used in the experiments. In the first case, the Hooke's law and the standard procedure for signal processing in reflected and transmitted waves were used for constructing the stress–strain diagrams; in the second case, the viscoelastic SLS model and signal processing for three waves by general formulas (1)–(3) were applied.

Figure 4 shows the dynamic compression diagrams for D16 Duralumin in six experiments. Taking into account the statistical scatter and the errors of the split Hopkinson bar technique, the dynamic behavior of D16 Duralumin is almost identical for steel and Plexiglas bars used. However, the use of polymeric pressure bars requires a more complicated processing of strain signals from strain gauges. The dynamic strain curves plotted in Fig. 4 illustrate the repeatability of test results. The dynamic yield strength for D16 determined by these curves is (250 ± 20) MPa.

4. Determination of Dynamic Compression Diagrams for Highly Deformable Materials. To demonstrate the capabilities of the polymeric split Hopkinson bar technique, stress–strain curves were obtained for several materials with an acoustic impedance between 0.06 and 1.4 MPa · sec/m. The size of cylindrical specimens was chosen in accordance with recommendations of Davies and Hunter [9]: diameter $D_{\rm s} = 4$–12 mm and length $l_{\rm s} = 2$–6 mm for $l_{\rm s}/D_{\rm s} \approx 0.5$.

Spheroplastic. This material is a quasi-isotropic composite with an epoxy matrix and dispersed inclusions in the form of glass microspheres. The volume density of the material is 0.63 g/cm^3, and the static yield strength under compression is approximately 60 MPa. For this material, the stress–strain diagrams were obtained on steel and Plexiglas bars for a loading pulse duration of about 150 μsec and a strain rate of (3000 ± 300) sec^{-1} (Fig. 5). Good agreement of the results is observed for strains lower than 10%. The data confirm the previously noted 1.5-fold increase in the yield strength in dynamic compression [12]. The transition to the state of forced elasticity is also observed at $\varepsilon > 4$–6%. The compression curve has practically no differences from that determined previously for $\varepsilon < 15$% on steel pressure bars, which testifies to the reliability of results obtained on Plexiglas bars. At the same time, it was possible to significantly expand the range of strains (up to 40%).

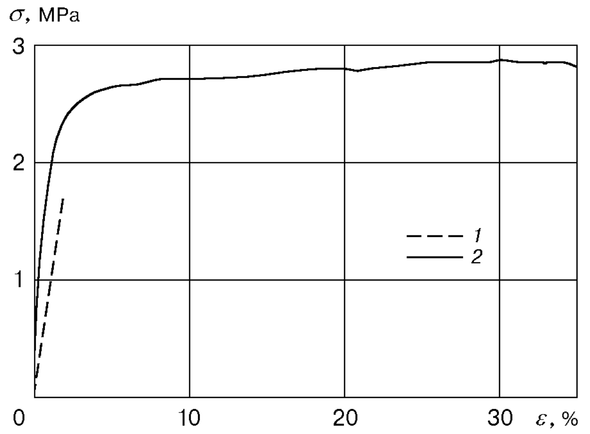

Fig. 6

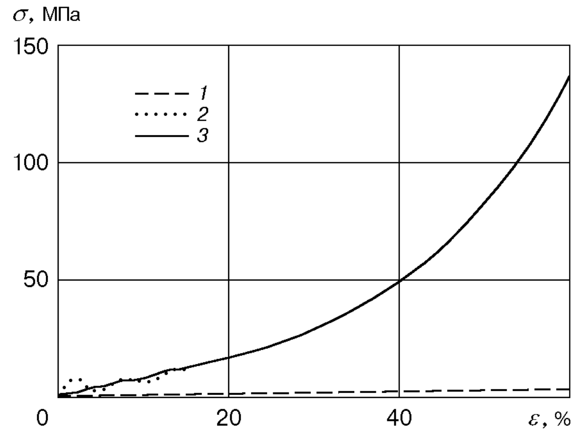

Fig. 7

Fig. 6. Static (1) and dynamic (2) stress–strain curves for PVC foam plastic ($I = 0.05$ MPa · sec/m and $\rho = 0.1$ g/cm^3) obtained with the use of Plexiglas bars.

Fig. 7. Static (1) and dynamic compression curves for rubber ($I = 0.06$ MPa·sec/m and $\rho = 1.2$ g/cm^3) obtained using pressure bars made of steel (2) and Plexiglas (3).

PVC Foam Plastic. The compression curve for low-density (approximately 0.1 g/cm^3) foam plastic demonstrates most clearly the capability of the technique (Fig. 6). The measured yield strength for a strain rate of 3000 sec^{-1} is 2.6 MPa, which exceed the value of 1.5–2 MPa obtained in static tests [10]. The stress–strain diagram of foam plastic cannot be determined with the use of metallic pressure bars because of the low amplitude of the transmitted wave.

Technical Rubber. This material with a density of 1.2 g/cm^3 was chosen as an example of a highly deformable material with low values of the velocity of sound (approximately 50 m/sec) and modulus of elasticity. The compression diagram indicates a high sensitivity of the stress–strain curve of the material to the strain rate (Fig. 7). Thus, in the case of static tests, the elasticity modulus of rubber under compression is 3–5 MPa [10]. The value of the elasticity modulus in dynamic tests (being determined by the slope of the part of the strain curve for $\varepsilon \leqslant 10\%$) for a strain rate of 3000 sec^{-1} reaches 100 MPa, which is at least 20 times greater than the static value. Rubber seems to be an example of a material with the stress–strain diagram highly sensitive to the strain rate. This result correlates qualitatively with the significant change in the elasticity modulus from 25 to 9000 MPa for rubber deformed in quasi-static compression tests at an ambient hydrostatic pressure of 5–10 kbar [13]. According to the generic principle of the temperature–time analogy, an increase in the strain rate is qualitatively equivalent to a decrease in the test temperature or to an increase in the ambient static pressure. This leads to a decrease in mobility of the main structural components of the material, which is responsible for the drastic increase in the elasticity modulus of the material.

It should be noted that high compression strains require a correction (namely, decrease) of stresses because of the increase in the cross-sectional area of the specimen of the material examined in the course of compression. This was not done at this stage of research, since it was not clear how the high strain rate affects the Poisson's ratio in homogeneous materials and whether the destruction of the solid skeleton of porous materials occurs with subsequent packing of the material in compression without significant increase in the specimen diameter. Nevertheless, the qualitative character of dynamic curves in compression does not change if this correction is applied.

Conclusions. Within the framework of the standard linear solid model, a technique for reconstruction of the profiles of strain, particle velocity, and stress in an arbitrary cross section of a viscoelastic bar on the basis of the strain signal registered in one section is developed. The good quantitative agreement of experimental and calculated strain profiles allows us to state that the SLS model is adequate to the problem considered and to the chosen material of pressure bars. This model may be used to reconstruct velocity and stress histories at the ends of the specimen of the material examined, which are necessary for calculation of the stress–strain diagram on the basis of the split Hopkinson bar technique. The reliability of this technique is confirmed by determining the dynamic diagram for D16 Duralumin with the use of polymeric and steel pressure bars. The capabilities of the technique are demonstrated by examples of determining stress–strain data in compression for low-density low-strength highly deformable materials (spheroplastic, PVC foam with a density of 0.1 g/cm^3, and technical rubber) with an acoustic impedance of 0.05–1.4 MPa $\cdot$ sec/m and characteristic stresses of 1–100 MPa and strains up to 50%.

The authors are grateful to A. V. Plastinin for his assistance in preparing and conducting experiments at the initial stage of work.

This work was supported by the Russian Foundation for Fundamental Research (Grant Nos. 99-01-00516 and 00-15-96181) and Federal Goal-Oriented Program "State Support of Integration of Higher Education and Fundamental Science for 1997–2000" (Grant No. 274).

REFERENCES

1. G. Kolsky, *Stress Waves in Solids*, Oxford (1953).
2. R. M. Davies, *Stress Waves in Solids*, Cambridge (1956).
3. T. Nikolas, "Behavior of materials at high rates of strain," in: J. Zykas et al. (ed.), *Impact Dynamics*, Wiley, New York (1982).
4. A. M. Bragin, "Experimental analysis of the processes of deformation and failure of materials under strain rates of 10^2–10^5 sec^{-1}," Author's Abstract, Doct. Dissertation in Tech. Sci., Nizhnii Novgorod University, Nizhnii Novgorod (1998).
5. K. Labibes, L. Wang, and G. Pluvinage, "On determining the viscoelastic constitutive equation of polymers at high strain-rates," *DYMAT J.*, **1**, No. 2, 135–151 (1994).
6. L. Wang, K. Labibes, Z. Azari, and G. Pluvinage, "Generalization of split Hopkinson bar technique to use viscoelastic bars," *J. Impact Eng.*, **15**, No. 5, 669–686 (1994).
7. O. Sawas, N. S. Brar, and A. C. Ramamurthy, "High strain rate characterization of plastics using polymeric split Hopkinson bar," in: S. C. Schmidt and W. C. TaoShock (eds.), *Shock Compression of Condensed Matter-1995*, Part 1, Amer. Inst. Phys., New York (1995), pp. 581–584.
8. O. Sawas, N. S. Brar, and R. A. Brockman, "High strain rate characterization of low-density low-strength materials," in: S. C. Schmidt, D. P. Dandekar, and J. W. Forbes (eds.), *Shock Compression of Condensed Matter-1997*, Amer. Inst. Phys., New York (1997), pp. 855–858.
9. E. D. Davies and S. C. Hunter, "The dynamic compression testing of solids by the method of the split Hopkinson pressure bar," *J. Mech. Phys. Solids*, **11**, 155–178 (1963).
10. V. A. Popov (ed.), *Materials in Machine Building*, Vol. 5: *Nonmetallic Materials* [in Russian], Mashinostroenie, Moscow (1969).
11. C. W. Curtis, "Propagating of an elastic strain pulse in a semi-infinite bar," in: D. Norman (ed.), *Proc. Int. Symp. on Stress Waves Propagation in Material*, Interscience Publ., New York (1960), pp. 15–43.
12. A. V. Plastinin, V. V. Sil'vestrov, and N. N. Gorshkov, "Determination of the dynamic compression diagram of spheroplastic," *Mekh. Kompoz. Mater.*, No. 3, 451–454 (1990).
13. C. W. Weaver and M. S. Paterson, "Stress–strain properties of rubber at pressures above the glass transition pressure," *J. Polymer Sci.*, **7**, Part A-2, No. 3, 587–591 (1969).